Numerical simulation of the fractional flow reserve (FFR)

Keltoum Chahour, Rajae Aboulaich, Abderrahmane Habbal, Cherif Abdelkhirane, Nejib Zemzemi

Math. Model. Nat. Phenom.
https://doi.org/10.1051/mmnp/2018069

Mathematical Modelling of Natural Phenomena
www.mmnp-journal.org

NUMERICAL SIMULATION OF THE FRACTIONAL FLOW RESERVE (FFR)

Keltoum Chahour[1,2], Rajae Aboulaich[1,3,*], Abderrahmane Habbal[2], Cherif Abdelkhirane[4] and Nejib Zemzemi[5,3]

Abstract. The fractional flow reserve (FFR) provides an efficient quantitative assessment of the severity of a coronary lesion. Our aim is to address the problem of computing non-invasive virtual fractional flow reserve (VFFR). In this paper, we present a preliminary study of the main features of flow over a stenosed coronary arterial portion, in order to enumerate the different factors affecting the VFFR. We adopt a non-Newtonian flow model and we assume that the two-dimensional (2D) domain is rigid in a first place. In a second place, we consider a simplified weakly coupled FSI model in order to take into account the infinitesimal displacements of the upper wall. A 2D finite element solver was implemented using Freefem++. We computed the VFFR profiles with respect to different lesion parameters and compared the results given by the rigid wall model to those obtained for the elastic wall one.

Mathematics Subject Classification. 35Q30, 92C50, 97M60, 74F10.

Received 08 February 2018. Accepted 07 November 2018.

1. Introduction

Atherosclerosis is a chronic inflammatory disease that affects the entire arterial network and especially the coronary arteries. It is an accumulation of lipids over the arterial surface due to a dysfunction of this latter. The objective of clinical intervention, in this case, is to establish a revascularization using different angioplasty techniques, among which the implantation of stents is the most widespread. This intervention involves introducing a stent into the damaged portion in order to allow the blood to circulate in a normal way over all the vessels. Revascularization is based on the principle of remedying ischemia, which is a decrease or an interruption of the supply of oxygen to the various organs. This anomaly is attenuated by the presence of several lesions (multivessel disease patients), which can lead to several complications. The key of a good medical intervention is the fact of establishing a good diagnosis, in order to decide which lesion requires to be treated. In the diagnosis

Keywords and phrases: Atherosclerosis, fractional flow reserve, generalized flow model, fluid–structure interaction.

[1] LERMA, Mohammadia Engineering School, Mohamed V University, Rabat, Morocco.
[2] Université Côte d'Azur, Inria, CNRS, LJAD, UMR 7351, Parc Valrose, 06108 Nice, France.
[3] International Laboratory for Computer Sciences and Applied Mathematics LIRIMA.
[4] Clinique Maarif - Cardiologie maarif, 20390 Casablanca, Morocco.
[5] INRIA Bordeaux Sud Ouest, Carmen Project, France.

* Corresponding author: aboulaich@gmail.com

Article published by EDP Sciences

phase, the clinician uses several techniques, among which angiography is the most popular. Angiography is an X-ray technique to show the inside (the lumen) of blood vessels, in order to identify vessel narrowing: stenosis. Despite its widespread use, angiography is often imperfect in determining the physiological significance of coronary stenosis. If the problem remains simple for non-significant lesions ($\leq 40\%$) or very severe ($\geq 70\%$), a very important category of intermediate lesions must benefit from a functional evaluation which will determine the strategy of treatment [6].

The technique of the fractional flow reserve (FFR) has derived from the initial coronary physical approaches decades ago. Since then, many studies have demonstrated its effectiveness in improving the patients prognosis, by applying the appropriate approach. Its contribution in the reduction of mortality was statistically proved by the Fractional Flow Reserve Versus Angiography for Multivessel Evaluation (FAME) study [16]. It is established that the FFR can be easily measured during coronary angiography by calculating the ratio of distal coronary pressure P_d to aortic pressure P_a. These pressures are measured simultaneously with a special guide-wire. FFR in a normal coronary artery equals to 1.0. FFR value of 0.80 or less identifies ischemia-causing coronary lesions with an accuracy of more than 90% [16].

Obviously, from an interventional point of view, the FFR is binding since it is invasive. It should also be noted that this technique induces additional costs, which are not covered by insurances in several countries. For these reasons, it is used only in less than 10% of the cases.

In this perspective, a new virtual version of the FFR, entitled virtual fractional flow reserve (VFFR), has emerged as an attractive and non-invasive alternative to standard FFR, see [12, 15]. However, there are key scientific, logistic and commercial challenges that need to be overcome before VFFR can be translated into routine clinical practice.

Blood circulation is generated by the heart "pump" that produces consecutive contraction/relaxation movements. These movements are performed during what we call a cardiac cycle. It consists of two phases: the systole, that is the phase of contraction. It occupies about one third of the cardiac cycle. The diastole, during which the heart muscle relaxes and refills with blood. It lasts the two remaining thirds of the cardiac cycle. Assuming a healthy heart and a typical rate of 70–75 beats per minute, each cardiac cycle takes about 0.8 sec. A flow and pressure wave starts from the heart to cross all major arteries in which it is damped, dispersed and reflected due to changes in vessel sizes, as well as the properties of the tissues and branches. The two coronary arteries cover the surface of the heart and represent the first derivations of the general circulation, see Figure 1.

1.1. Fractional flow reserve

In order to provide a good estimation of the VFFR, a good understanding of the FFR technique as well as the various medical verifications preceding the test is required. In this section, we give details about the invasive FFR. The patient is initially placed in the supine position. To start the measure of the FFR the operator crosses the coronary lesion with an FFR-specific guide wire. This guide wire is designed to record the coronary arterial pressure distal to the lesion (Fig. 2 left). Once the transducer is distal to the lesion (approximately 20 mm), a hyperemic stimulus is administered by injection through the guide catheter, and here the FFR value is subject to a wide variation. The operator waits for few minutes so that the FFR value becomes constant, this value corresponds to the maximal vasodilatation.

The mean arterial pressures from the pressure wire transducer P_{aortic} and from the guide catheter P_{distal} are then used to calculate FFR ratio: $\text{FFR} = P_{\text{distal}}/P_{\text{aortic}}$ (Fig. 2 right).

The pressure values given by the FFR instrument are calculated as temporal mean pressures over small time intervals, depending on the frequency of acquisition of the pressure sensor $p_s(t)$. Assuming that T_c is the duration of a cardiac cycle, these pressures are given as follows:

$$P = \frac{1}{T_c} \int_0^{T_c} p_s(t) dt. \tag{1.1}$$

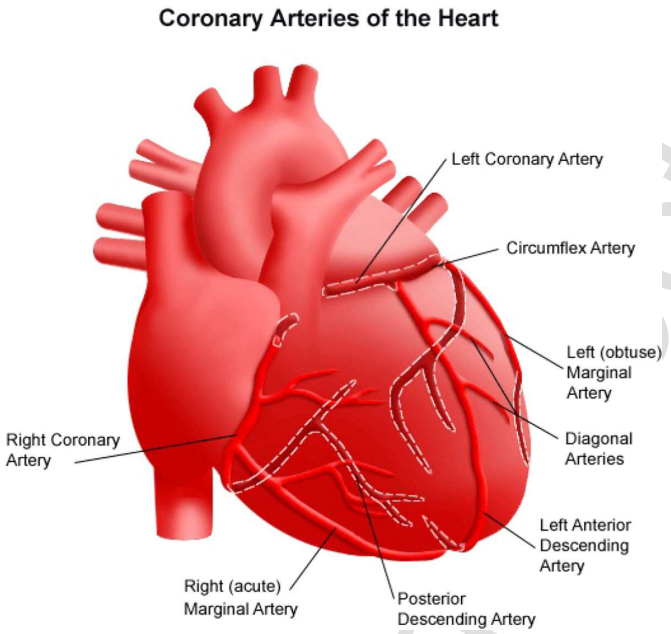

FIGURE 1. The coronary tree [19].

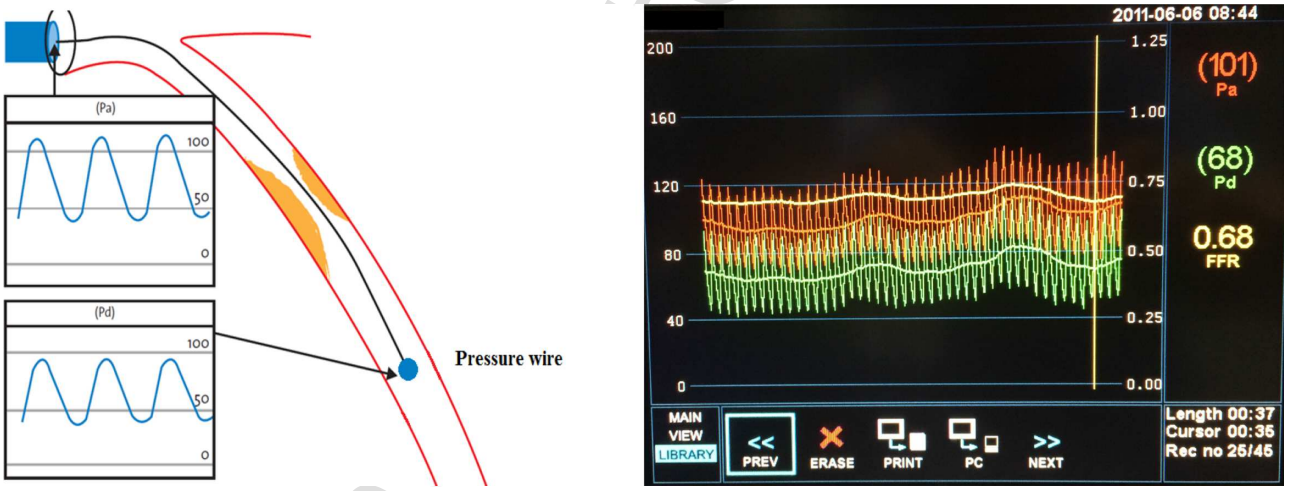

FIGURE 2. Left, represents schema of the invasive FFR technique [6]. Right, a typical example of FFR measurement. Automated calculation of FFR corresponds to the ratio of mean distal coronary pressure (green) to mean aortic pressure (red) during maximal hyperemia, see [14].

An FFR value lower than 0.75 indicates a hemodynamically significant lesion. An FFR value higher than 0.8 indicates a lesion that is not hemodynamically significant. Values between 0.75 and 0.80 are indeterminate and should be considered in the context of patient's clinical history to determine if revascularization is necessary.

Modeling and simulation of blood flow have attracted a lot of attention. A realistic modeling of blood velocity and pressure is mandatory in view of virtual design and analysis of the performance of some medical devices,

such as heart valves, filters and stents, on one hand. On the other hand, it provides clinicians with a set of non-invasive and reliable tools to guide the diagnostic phase.

In this paper, we aim at presenting a preliminary two-dimensional (2D)-based study to understand the flow distribution in a stenosed coronary artery and to enumerate the factors that affect the value of the VFFR. We give a special concern to the influence of the lesion's parameters.

Since we are interested in studying the flow in the coronary arteries, we decided to use a non-Newtonian flow model like in [3] and [2]. In fact, the coronary arteries have a small caliber (0.5 cm) compared to the aorta for example, where the use of non-Newtonian flow model is not really crucial. In a first place, we assumed that the arterial wall is rigid. This is justified by the fact that the FFR value taken into account by the clinician during the test is established into a domain corresponding to the maximal vasodilation.

In a second place, we considered a simplified weakly coupled fluid–structure interaction model to include the arterial wall elastic behavior, as presented in [7]. The coronary arteries are subject to two different displacements:

- Large displacements: Since they are partially attached to the myocardium, they are directly influenced by the myocardium contraction/relaxation, and by the movements induced by the respiratory system.
- Small displacements: Due to the propagation of the blood wave generated by the heart pulse.

In this work, we chose to restrain our study to the small displacements. Moreover, only the upper face of the arterial portion is involved since the lower one is fixed (glued to the myocardium), see [9]. We also assume that the displacements of the shell are infinitesimal. As for the boundary conditions, even if their choice is crucial for this kind of studies, we decided to make few simplifications in order to be able to address the problem. At the inlet, we impose a sinusol wave function to illustrate the pulsatile property of the flow, as in many works [8], [7] and [9]. At the outlet, we assume that the vessel following the portion of interest is long enough before getting to the small tissues, or having a change in the vessel caliber, so there is no resistance effect. This justifies the choice of natural outlet boundary condition.

We implement from scratch, within the FreeFem++ environment, a finite element solver for both the generalized flow model and the coupled arterial wall/blood flow model. To describe the 2D mobile domain, we used an Arbitrary Lagrangian–Eulerian (ALE) coupling scheme. Like in [9], we proceed by decoupling the problem into two parts: solid and fluid, while introducing coupling boundary conditions at the interface. We then introduce and implement an algorithm for computing the VFFR following the industrial manufacturer protocol for the analogic FFR estimation. Using the solvers, we lead a study of the VFFR with respect to the stenosis dimensioning parameters (degree of stenosis and lesion radius).

In this study, our goal is to provide a first estimation of the coronary fractional flow reserve VFFR in a simplified 2D geometry. We conduct different simulations in order to identify the impact of the lesion's parameters on the value of VFFR. In Section 1, we present the non-Newtonian flow model used to carry all the simulations, as well as the boundary conditions. In Section 2, we give some numerical results considering that the arterial portion is rigid. The flow and pressure distributions are given in two different geometries: a single stenosis case (presence of only one lesion), and a multi-stenosis case. In these two configurations of the domain, we plot VFFR variations according to some parameters of influence: degree of stenosis, lesion's radius and the spacing between the two lesions in the multi-stenosis case. In Section 3, we present the fluid–structure interaction model, and the different VFFR variations corresponding to it.

2. Generalized non-Newtonian flow model

In large arteries, blood flow can be modeled by the Navier–Stokes equation. In our case, the blood cannot be assimilated to a Newtonian fluid, since the coronary vessels caliber is very small (0.5 cm). We choose a non-Newtonian flow model, as in [3]. The mathematical model was studied in [3] and authors proved the existence of a solution to this type of problems. In this paper, we are more interested in giving a bi-dimensional based estimation of the VFFR on the one hand. On the other hand, we lead different simulations, in order to explore the impact of the plaque's characteristics on the velocity and pressure fields.

We consider the Carreau law and we suppose that the viscosity varies as a function of the second invariant of the deformation tensor $s(u)$:

$$(s(u))^2 = 2Du : Du = 2\sum_{i,j}(Du)_{ij}(Du)_{ji}, \tag{2.1}$$

with:

$$Du = \frac{1}{2}(\nabla u + \nabla^T u). \tag{2.2}$$

Following the Carreau law, μ is given by:

$$\mu = \mu_\infty + (\mu_0 - \mu_\infty)(1 + (\lambda s(u))^2)^{(n-1)/2}, \tag{2.3}$$

where $\mu_0 = 0.0456$ Pa.s and $\mu_\infty = 0.0032$ Pa.s, are the values of the viscosity for the lowest and highest shear rates. $\lambda = 10.03$ s and $n = 0.344$.

The problem considered involves the blood velocity $u = (u_1, u_2)$ and pressure p defined in $\Omega_f \times (0, T_c)$ as follows (the considered domain Ω_f is shown in Fig. 3):

$$\begin{cases} \rho_f \dfrac{\partial u}{\partial t} + \rho_f (u.\nabla)u - \nabla.(2\mu(s(u))Du) + \nabla p = 0, \ \ sur \ \ \Omega_f \times (0, T_c) \\ \nabla.u = 0, \ \ sur \ \ \Omega_f \times (0, T_c) \end{cases} \tag{2.4}$$

where ρ_f is the blood density, we impose $\rho_f = 1060$ kg.m^{-3} like in [3, 7].

These equations are completed with the following boundary conditions on Ω_f (n is the normal):

$$2\mu(s(u))Du.n - pn = h, \ \ sur \ \ \Gamma_{\text{in}} \times (0, T_c), \tag{2.5}$$

$$2\mu(s(u))Du.n - pn = 0, \ \ sur \ \ \Gamma_{\text{out}} \times (0, T_c), \tag{2.6}$$

$$u = 0, \ \ sur \ \ \Gamma_{\omega_1} \cup \Gamma_{\omega_2} \times (0, T_c). \tag{2.7}$$

The blood flow is initially at rest and enters the vessel by the left side Γ_{in} where a sinusol pressure-wave with a maximum $P_{\max} = 10^4$ Pa is prescribed during $T^* = 5.10^{-3}$ sec. The wave's profile is set equal to a stress vector of magnitude h, oriented in the negative normal direction given by the equation:

$$h = \begin{cases} (P_{\max} \times (1 - \cos(2\pi t/T^*)), 0)^t, x \in \Gamma_{\text{in}}, \ \ 0 \ \ \leq t \leq T^* \\ (0,0)^t, \qquad\qquad\qquad\qquad x \in \Gamma_{\text{in}}, \ \ T^* \leq t \leq T_c. \end{cases} \tag{2.8}$$

We consider that the fixed geometry at $t = 0$ corresponds to a maximal vasodilation.

The outflow is the right boundary Γ_{out} where a zero pressure is imposed. A no-slip condition is enforced on the lower and upper boundaries Γ_{ω_1} and Γ_{ω_2}, which assume that the fluid is not moving with respect to these boundaries.

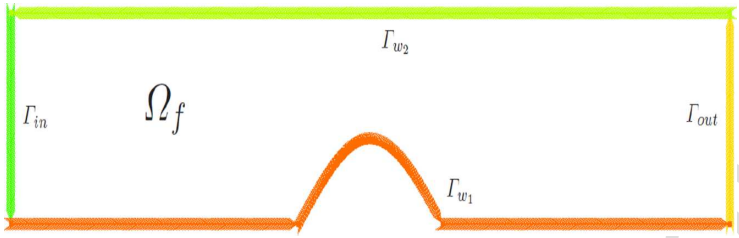

FIGURE 3. Considered geometry for the problem.

The initial condition is the solution of a steady Stokes problem with a Poiseuille flow profile at the inlet, given by the following equation:

$$u_0(y) = u_{0m} \times y/H \times (1 - y/H), \tag{2.9}$$

where $u_{0m} = 0.4$ m/s.

Arterial coronary plaques present a large variability in their configuration. We chose a simplified axisymmetric 2D configuration in order to address our problem, following [9]. The shape of the plaque in this case is modeled as a sinusol function:

$$\omega_s(x) = \begin{cases} D \times \cos(\pi(x - x_s)/2 * \delta) \text{ if } x_s - \delta < x < x_s + \delta \\ 0 \qquad\qquad\qquad\qquad\qquad\qquad \text{otherwise.} \end{cases} \tag{2.10}$$

We consider a portion of a length $L = 60$ mm from the diseased artery. The lumen diameter is considered equal to $H = 5$ mm (coronary artery). The plaque is assumed to be 100% eccentric and it is characterized by three parameters: D the height of the plaque, x_s the position of the center of the plaque and $2 \times \delta$ its length. $R = D/H$ indicates the degree of stenosis, it varies by changing the value of D, see 3.

The variational formulation of the problem can be written as follows:

$$\begin{cases} \rho_f \displaystyle\int_{\Omega_f} \frac{\partial u}{\partial t} v dx + (Au, v) + \rho_f b(u, u, v) = \int_{\Gamma_{\text{in}}} hv d\sigma + \int_{\Gamma_{\omega_1}} gv d\sigma, \ \ \forall v \in V \\ u(0) = u_0, \ \ sur \ \ \Omega_f \end{cases} \tag{2.11}$$

with:

$$(Au, v) = \int_{\Omega_f} 2\mu(s(u)) Du : Dv dx, \tag{2.12}$$

$$b(u, v, w) = \sum_{i,j=1}^{2} \int_{\Omega_f} u_i \frac{\partial v_j}{\partial x_i} w_j dx. \tag{2.13}$$

Simulations are performed using the finite element solver Freefem++, based on a semi-implicit time discretization scheme. Fluid velocity and pressure are calculated at each time step. A comparison with the Newtonian

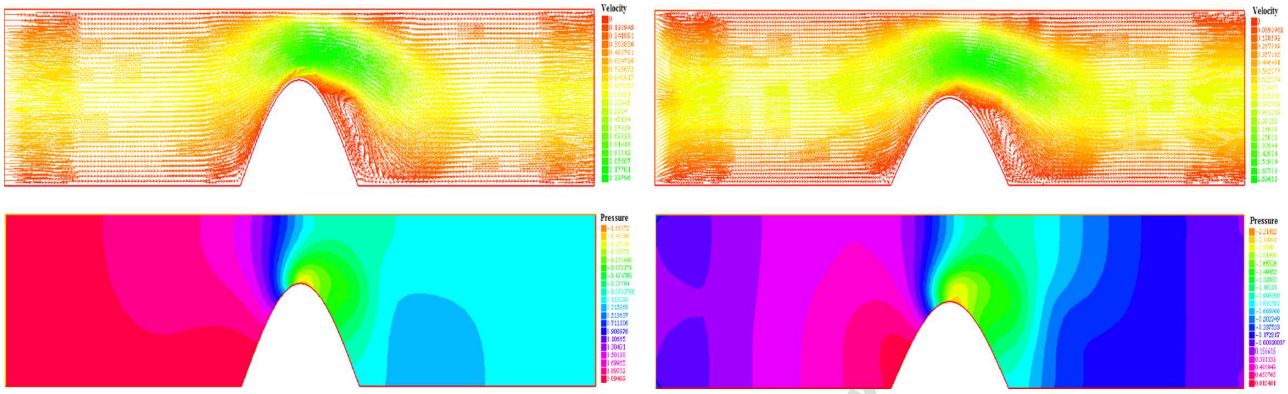

FIGURE 4. Left, velocity and pressure field with Navier–Stokes equation at time $t = 0.3\,\mathrm{s}$. Right, velocity and pressure field with the generalized flow model at time $t = 0.3\,\mathrm{s}$.

flow is established for both the blood velocity and pressure. The time step is $\delta t = 5.10^{-3}\,\mathrm{s}$ and the duration of a cardiac cycle is $T_c = 0.8$ s. Five consecutive cardiac cycles were simulated to ensure that the flow was truly periodic. To confirm the independence of the numerical solutions on the space discretization, computations were repeated for different mesh sizes.

In order to visualize the impact of the plaque's characteristics on the flow over the diseased portion of the artery, the degree of stenosis R varies from 40% to 70% (focusing only on the intermediate lesions). The plaque's radius also varies from 2.5 mm to 5 mm. Since the presence of many lesions is clinically frequent, we have also considered a geometrical model with two plaques to get an estimation of the velocity and pressure field variations in this case.

3. NUMERICAL RESULTS

3.1. The case of single stenosis

The simulation of blood flow in the presence of stenosis in a 2D geometry has been the subject of several works [3, 9, 10]. These works were based on the Navier–Stokes model and the arterial wall was considered to be rigid. In our work, we consider a non-Newtonian flow model, as in [3]. In this first simulation, the arterial wall is considered to be rigid. In Figure 4, we give velocity and pressure distribution using Navier–Stokes model, in a first place, and using the generalized flow model in the second. The length of the plaque is 10 mm, and the degree of stenosis is 40%. Velocity arrows show the flow profile across the portion of the vessel. We can see reverse flow on the distal side of the plaque. Severe stenosis leads to high flow velocity, high pressure at the throat of the lesion, and a large re-circulation region distal to it.

For the calculation of the VFFR ratio, the aortic pressure P_a is calculated at each time step by the spatial mean pressure of the nodes at 1 cm from the inlet of the vessel: $x_a = 1$ cm. Whereas the distal pressure P_d is obtained at 1 cm after the lesion: $x_d = x_s + 1$ cm. Then a temporal mean is performed during the cardiac cycle: mean P_a and mean P_d are then used to calculate the VFFR ratio. The following setting (Fig. 5) describes the approach.

In order to take into account the time variations in the value of the VFFR, this value is calculated during 5 consecutive cardiac cycles. We notice that starting from the third cardiac cycle, this value becomes constant. The VFFR takes values in the neighborhood of 0.67 for a lesion with a degree of stenosis equal to 75%.

The following graphic (Fig. 6) gives the variation of the VFFR during the five cardiac cycles.

For all the graphics in the next sections, the VFFR value considered is calculated during the third cycle of the simulation. The two preceding cycles are run in order to reach stable pressure distribution.

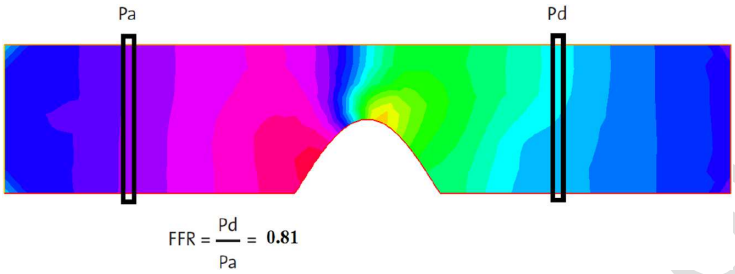

FIGURE 5. FFR calculation. In this case, the degree of stenosis is equal to 40% and the VFFR is equal to 0.81.

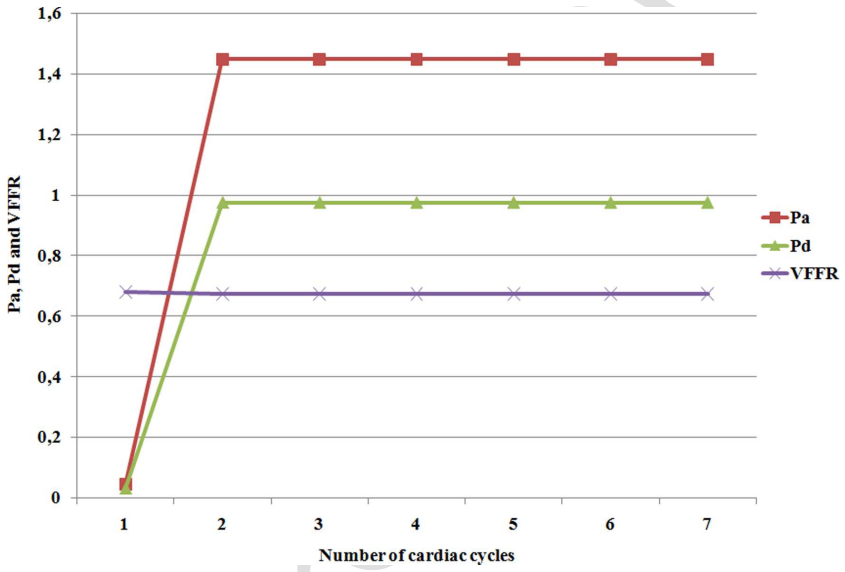

FIGURE 6. VFFR variation during 5 cardiac cycles for a lesion with 75% stenosis.

The following figures give the aortic pressure P_a, the distal pressure P_d and the VFFR respectively according to the degree of stenosis (Fig. 7 left) and the plaque's radius (Fig. 7 right).

The most common parameter considered to evaluate the significance of a lesion is the degree of stenosis. However, the lesion length (or radius) is also significant for this evaluation, especially when the degree of stenosis is in the intermediate value range [11]. The linear regression models presented in [11] give the correlation between the FFR value (obtained after the invasive test) and different plaque's parameters. Particularly, the lesion radius and the degree of stenosis were considered. The graphics given in paper [11] were obtained from a statistical study of medical data. The results in Figure 7 cannot be quantitatively compared to those presented in this paper; however, we can see qualitatively that the graphics have approximately the same trend.

Figure 8 shows the simulated VFFR corresponding to different values of the lesion radius according to the degree of stenosis. We can note from this figure that the curve describing the VFFR according to the degree of stenosis changes with the value of the lesion's radius. Thus, there is an important change in classification, especially for the lesions with a degree of stenosis lower than 45%. For example, for a degree of stenosis of 40%, VFFR value is equal to 0.82 in the case of a lesion's radius of 0.25 cm, and to 0.75 in the case of a lesion's radius of 0.5 cm. As a consequence, there is a change in the lesion's classification from not hemodynamically significant to hemodynamically significant.

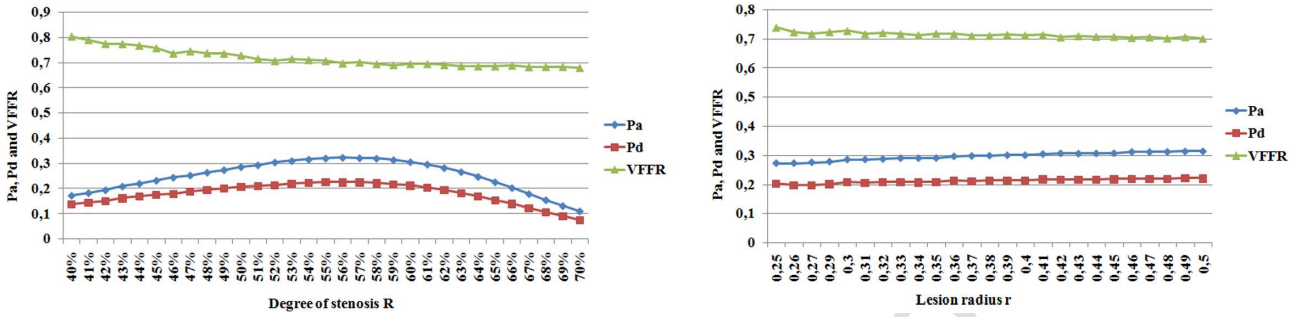

FIGURE 7. Left, P_a, P_d and VFFR variation according to the degree of stenosis R. Right, P_a, P_d and VFFR variation according to the lesion radius δ.

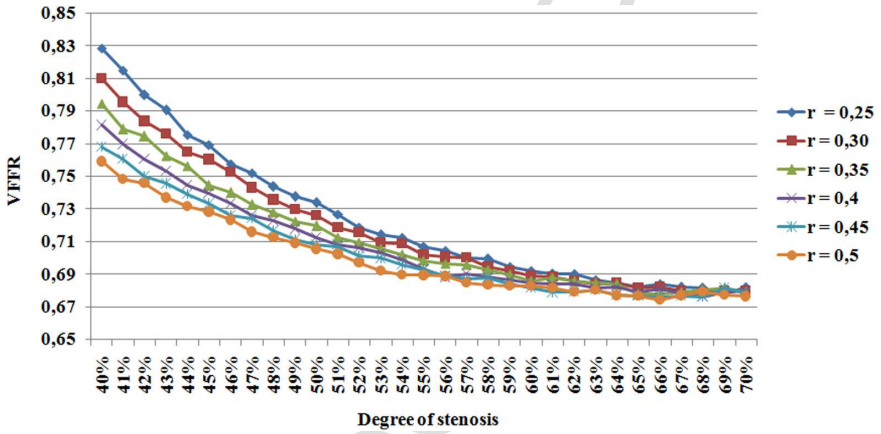

FIGURE 8. VFFR variation for lesions with different radius according to the degree of stenosis.

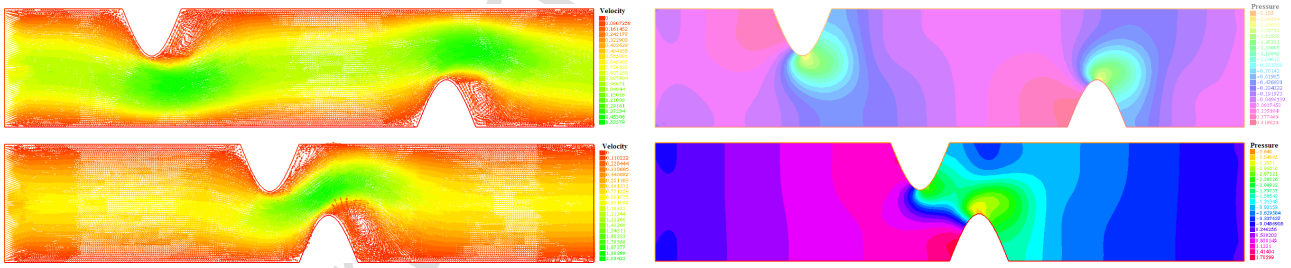

FIGURE 9. Top, velocity and pressure field corresponding to identic lesions of 40% stenosis, with a spacing 'a' of 0.5 cm. Bottom, velocity and pressure field with a spacing 'a' of 1.5 cm.

3.2. Mutli-stenosis case

In the case of a multi-stenosis diseased patient, many lesions might be considered in the arterial wall. The following figures describe the blood velocity and pressure in this case.

The distance between the two lesions influences the flow, and particularly the micro-circulation downstream of the stenosis. Thus, the values of the VFFR obtained in the two cases given in Figure 9 are different, even

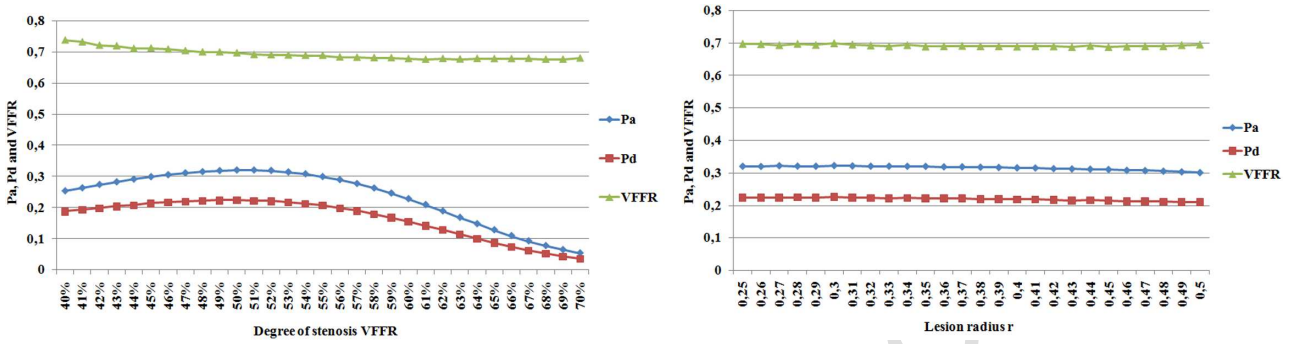

FIGURE 10. Left, P_a, P_d and VFFR variation according to the degree of stenosis R in the case of multiple stenoses. Right, P_a, P_d and VFFR variation according to the lesion radius δ in the case of multiple stenosis.

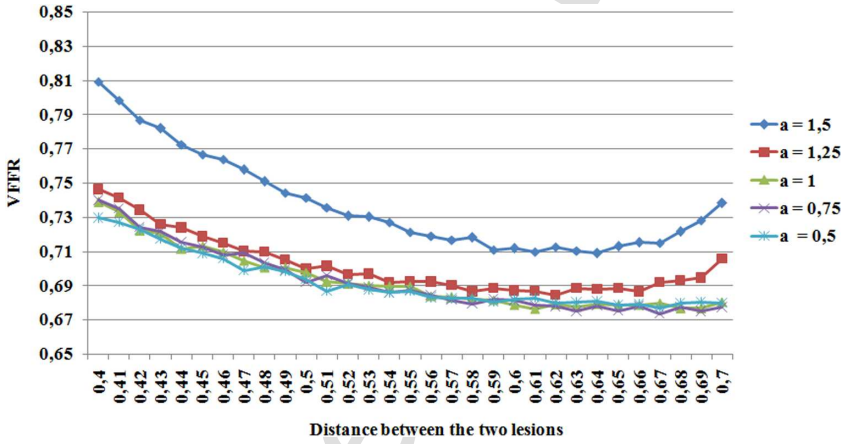

FIGURE 11. VFFR variation in the case of two identic lesions, with different spacings according to the degree of stenosis.

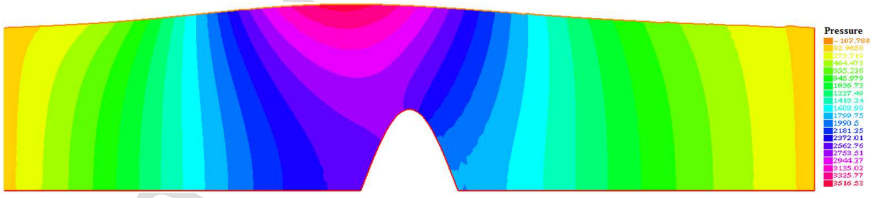

FIGURE 12. Pressure profile with the fluid–structure interaction model.

if the lesion is somehow similar. The VFFR obtained for a spacing of 0.5 cm is equal to 0.73, while the VFFR with a spacing of 1.5 cm is equal to 0.81.

4. COUPLING SCHEME: FLUID–STRUCTURE INTERACTION

To achieve more realistic simulations, we consider the fluid–structure interaction between the arterial wall and the blood. We assume that the displacements of the shell are infinitesimal, and that only the upper face

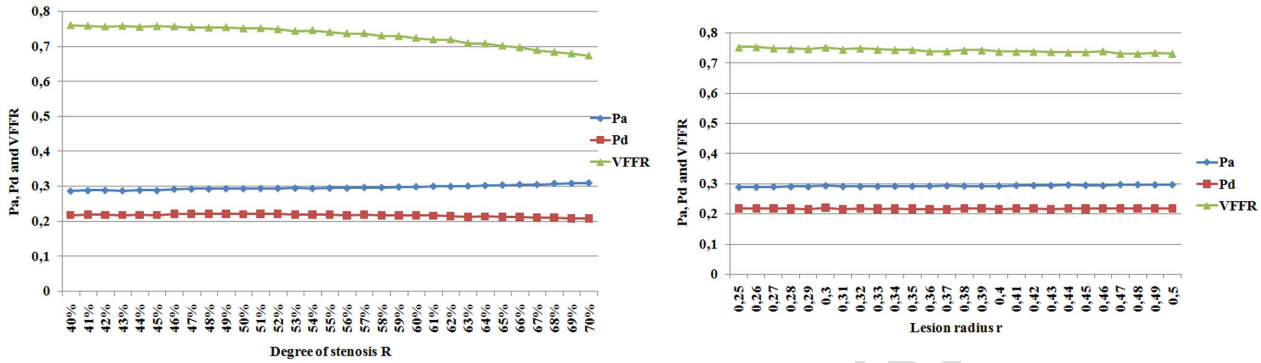

FIGURE 13. Left, P_a, P_d and VFFR variation according to the degree of stenosis R using the fluid–structure interaction model. Right, P_a, P_d and VFFR variation according to the lesion radius δ using the fluid–structure interaction model.

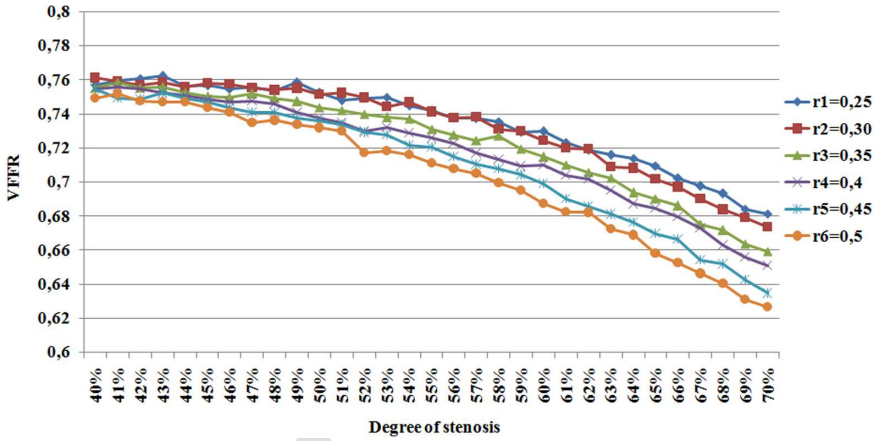

FIGURE 14. VFFR variation using the fluid–structure interaction model according to the degree of stenosis.

of the arterial portion is able to move. In a first place, a generalized linear Koiter model is adopted for the structure, as in [8]. In this case, the arterial wall is a 1D layer with a thickness ϵ.

The problem is to find the solid vertical displacement η and the solid vertical velocity $\dot{\eta} = \partial_t \eta$ of the solid such that:

$$\begin{cases} \rho_s \epsilon \partial_t \dot{\eta} - c_1 \partial_x^2 \eta + c_0 \eta = -\sigma(u,p)n.n & \text{over} \Gamma_{\omega_1} \times (0, T_c), \\ \dot{\eta} = \partial_t \eta & \text{over } \Gamma_{\omega_1} \times (0, T_c), \\ u.n = \dot{\eta}, u.\tau = 0 & \text{over } \Gamma_{\omega_1} \times (0, T_c), \\ \eta = 0 & \text{over } \partial\Gamma_{\omega_1} \times (0, T_c). \end{cases}$$

where:

$$\sigma(u,p) = -pI + 2\mu(s(u))Du.$$

u and p are respectively the fluid velocity and pressure, solutions of problem (2.4). $\rho_s = 1.1$ is the solid density. c_1 and c_0 are defined by: $c_1 = \frac{E\epsilon}{2(1+\nu)}$ and $c_0 = \frac{E\epsilon}{R^2(1-\nu^2)}$, solid thickness $\epsilon = 0.1$, Young modulus $E = 0.75 \times 10^6$ and Poisson coefficient $\nu = 0.5$.

The fluid–structure interaction model gives different results compared to the one with rigid boundaries (presented in Sect. 2). Therefore, we obtain different values for the VFFR. It should be expected that this model gives better values since it is more adapted to the physiology of the arterial wall. However, to validate the values obtained using this model, we should consider a realistic geometry, reconstructed from clinical images.

5. Conclusions

In this paper, we led different simulations to study the flow through a sclerotic artery. Firstly, we considered a generalized flow model in a fixed 2D domain. We assumed that the initial configuration of the domain corresponds to the maximal vasodilation of the portion of interest. Our purpose was to give a first estimation of the VFFR. We studied the variation of the VFFR with respect to some lesion's parameters: the degree of stenosis and the lesion's radius in the case of a single stenosis. In the case of multi-stenosis (the presence of two parallel lesions), we also studied the VFFR variations according to the distance between the two lesions, since this value also modifies the blood circulation through the diseased portion. Secondly, we introduced a generalized fluid–structure interaction model, in order to take into account the infinitesimal displacements of the upper arterial wall. Large displacements due to the myocardium movements were not considered. Each one of these models: rigid and elastic has a particular importance in the quantification of the VFFR. In medical practice, it is not the degree of stenosis that modifies the FFR value, even if this parameter is dominant to judge the severity of a lesion. But it is the coronary micro-circulation downstream of the stenosis and its importance that must impact the FFR. This micro-circulation depends not only on the shape of the plaque (flattened, large, sharp...), but also on the flow and the wall properties as well. The VFFR model presented in this paper is able to take into account modifications of the shape of the lesions, through certain parameters on the one hand. On the other hand, it is able to take into account/or not the elastic behavior of the upper wall. We highlight that the rigid model, fitted with patient-specific flow parameters, can give useful VFFR estimation in the case of non-viable vessels, while the elastic model, in general, is supposed to be more adapted to estimate the VFFR. The values of VFFR obtained by this model are certainly different from those obtained by the rigid one. This could be explained by the fact that the elastic property of the upper wall compensates the over-pressure before the lesion and thus modifies the pressure distribution in the whole domain.

The numerical results for the VFFR presented in this paper are not yet clinically usable. However, the aim is to enumerate some of the factors influencing the FFR value and to insist on the necessity of going beyond the degree of stenosis in the evaluation of a lesion. In this view, from the comparison between the Figures 8 and 14 we can conclude that the VFFR decreases with the degree of stenosis for both rigid and elastic models. As for the lesion's radius, it influences the VFFR in the rigid model only for lesions with a degree of stenosis lower than 60%. Beyond this value, the VFFR is not subject to a big change using this model. On the contrary, for the elastic model, the lesion's radius influences the VFFR for lesions with degree of stenosis higher than 50%. The geometry of the lesion, dimensioned by the two parameters: R the degree of stenosis and r the lesion's radius, affects the flow through the lesion, and depending on whether the domain is rigid or elastic, the pressure distribution is modified, and the VFFR variation as well.

Our aim for future works is to compare the results from modeling with *in vivo* measurements recorded during an interventional procedure based on 2D or 3D geometries issued from image reconstruction techniques. There are different approaches to reconstruct 3D vessels from 2D images. The most widespread are those that are based on images corresponding to different slices of the 3D object: mainly CT scans or MRI. Another 3D reconstruction technique is based on different projections of the 3D vessel, issued from 2D angiography, like presented in [12] and [18]. The choice of suitable conditions is crucial in order to obtain a good estimation of the VFFR. In this work, we chose simplified boundary conditions. Various studies have tackled the problem of boundary conditions in the case of blood flow like [13], [8] and [17]. In the case of complex geometries, or 3D domains reconstructed from medical imaging, there are several evacuations. This produces a resistant effect

at the exit due to the change in the vessels caliber, bifurcations and the variation in the properties of the wall. Therefore, the boundary conditions based on impedance and resistance models, commonly known in the literature as the Winkessel effect [4], are the most adapted to incorporate this reflected wave effect into the model [17].

The goal of this prospective study is to obtain a mathematical model integrating measurable clinical parameters with simulation performances which gives a very close estimation to the realistic FFR measure. The validation method of this calculation usually consists on matching the values resulting from simulation with those of the clinical invasive FFR test. That gives rise to a statistical study, as in [12] and [11]. Finally, FFR simulation in the cath lab could be a helpful tool for cardiologists, since it provides essential information during the coronary intervention. For this reason, FFR simulation should help in improving decision making as well as the prognosis of patients.

Acknowledgements. This work has been supported by EPICARD cooperative research program, funded by the INRIA international laboratory LIRIMA.

References

[1] C. Bertoglio, Forward and inverse problems in fluid-structure interaction. Application to Hemodynamics, in *Numerical Analysis*. Université Pierre et Marie Curie - Paris VI (2012).

[2] S. Boujena, N. El Khatib and O. Kafi, Generalized Navier-Stokes equations with Non-standard conditions for blood flow in atherosclerotic artery. *Appl. Anal.* **95** (2016) 1645–1670.

[3] S. Boujena, O. Kafi and N. El Khatib, A 2D mathematical model of blood flow and its interactions in an atherosclerotic artery. *Math. Model. Nat. Phenom.* **9** (2014) 32–54.

[4] M. Catanho, M. Sinha and V. Vijayan, Model of aortic blood flow using the Windkessel effect. in *Report BENG 221 – Mathematical Methods in Bioengineering*, October 2012.

[5] V. Chabannes, G. Pena and C. Prud'Homme, High-order fluid-structure interaction in 2D and 3D. Application to blood flow in arteries. *J. Comput. Appl. Math.* **246** (2013) 1–9.

[6] T. Cuisset, J. QuiliCi and G. Cayla, Qu'est-ce que la FFR? Comment l'utiliser? *Réalités Cardiologiques*, Janvier/Février 2013.

[7] M. Fernandez, M. Landajuela and M. Vidrascu, Fully decoupled time-marching schemes for incompressible fluid/thin-walled structure interaction. *Physics* **297** (2015) 156–181.

[8] P. Gostaf and O. Pironneau, Pressure boundary conditions for blood flows. *Chin. Ann. Math. Ser. B* **36** (2015) 829–842.

[9] T. Lassila, A. Manzoni, A. Quarteroni and G. Rozza, A reduced computational and geometrical framework for inverse problems in haemodynamics. *Int. J. Numer. Methods Biomed. Eng.* (2013) 1–35.

[10] Z.-Y. Li, S.P.S. Howarth, T. Tang and J.H. Gillard, How critical is fibrous cap thickness to carotid plaque stability?: a flow-plaque interaction model. *Stroke* **37** (2009) 1195–1199.

[11] R. Lopez-Palop, P. Carrillo, P. Agudo, A. Frutos, A. Cordero, M. Lopez-Aranda, *et al.*, Correlation between intracoronary ultrasound and fractional flow reserve in long coronary lesions. A three-dimensional intracoronary ultrasound study. *Soc. Espan. Cardiol.* **66** (2013) 707–714.

[12] P.D. Morris, F.N. van de Vosse, P.V. Lawford, D. Rodney Hose and J.P. Gunn, Virtual (computed) fractional flow reserve: current challenges and limitations. *JACC Cardiovasc. Interv.* **8** (2015) 1009–1017.

[13] O. Pironneau, Simplified fluide-structure interactions for hemodynamics, in *Numerical Simulations of Coupled Problems in Engineering*. Springer Verlag (2014) 57–70.

[14] G. Toth, P. Johnson, A. Jeremias, M. Pellicano, P. Vranckx, F. Fearon *et al.*, Standardization of fractional flow reserve measurements. *J. Am. Coll. Cardiol.* **68** (2016) 742–753.

[15] S. Tu, E. Barbato, Z. Köszegi, J. Yang, Z. Sun, N.R. Holm *et al.*, Fractional flow reserve calculation from 3-dimensional quantitative coronary angiography and TIMI frame count. *JACC Cardiovasc. Interv.* **7** (2014) 768–777.

[16] L.X. van Nunen, R. Lycett, P.V. Lawford, R. Hose and J.P. Gunn, Fractional flow reserve versus angiography for guidance of PCI in patients with multivessel coronary artery disease (FAME): 5-year follow-up of a randomised controlled trial. *Lancet* **386** (2015) 1853–1860.

[17] I.E. Vignon-Clementel, C. Alberto Figueroa, K.E. Jansen and C.A. Taylor, Outflow boundary conditions for three-dimensional finite element modeling of blood flow and pressure in arteries. *Comput. Methods Appl. Mech. Eng.* **195** (2006) 3776–3796.

[18] J. Yang, Y. Wang, Y. Liu, S. Tang and W. Chen, Novel approach for 3-D reconstruction of coronary arteries from two uncalibrated angiographic images. *IEEE Trans. Image Process.* **18** (2009) 1563–1572.

[19] Available online from https: //stanfordhealthcare.org/content/dam/SHC/conditions/blood-heart-circulation/images/anomalouscoronaryartery-diagram-heart.gif.

Author Query

Q1 Please check the change made of full form of 'VFFR' for correctness.
Q2 Please provide the city and country name of affiliation 3.
Q3 Please provide the citation of Figs. 10–13 in text suitably.
Q4 Please verify the journal title, volume, year and page range of ref. [2].
Q5 Please verify the journal title, volume and page range of ref. [11].
Q6 Please check the author names of ref. [16].
Q7 Please check, refs. [13] and [18] are identical, so ref. [20] has been deleted from the list and text as well.
Q8 Please provide the access date of ref. [19].